Born Different: A Multi-Level Individualized Modeling Framework for Embryo Euploidy Prediction

Shuangyi Tan[1†] , Xinxian Song[2†], Qingyun Mai[3], Zhen Li[1*], Sibei Yang[2*] , Guanbin Li[2,4*]

[1] The Chinese University of Hong Kong, Shenzhen
[2] School of Computer Science and Engineering, Sun Yat-sen University
[3] The First Affiliated Hospital, Sun Yat-sen University
[4] Shenzhen Loop Area Institute
shuangyitan@link.cuhk.edu.cn, liguanbin@mail.sysu.edu.cn

Abstract. Accurate identification of euploid embryos is essential for improving outcomes in in vitro fertilization. While time-lapse imaging and deep learning enable non-invasive embryo assessment, most existing approaches model developmental sequences within a unified representation space, overlooking substantial inter-individual variability in morphology, developmental rhythm, and global developmental deviation. To address this limitation, we propose a **multi-level individualized modeling framework** that explicitly characterizes embryo variability from spatial, temporal, and global perspectives. First, at the morphological level, we characterize embryo-specific spatial heterogeneity by adaptively composing shared morphological components, enabling the model to preserve canonical structures while capturing individualized structural variations. Second, at the temporal level, we model individualized developmental dynamics by adaptively reweighting time points, allowing the framework to emphasize embryo-specific critical stages rather than enforcing uniform temporal importance. Third, at the global level, we incorporate reliability-aware modeling to explicitly characterize uncertainty and developmental deviation, balancing population-level regularities with individual-specificity. Extensive experiments demonstrate that the proposed method achieves state-of-the-art performance, highlighting the importance of explicitly modeling embryo individuality for euploidy prediction. The GitHub link is https://github.com/Renard131/MIEP.

Keywords: In Vitro Fertilization · Time-Lapse Video · Multimodal.

1 Introduction

In vitro fertilization (IVF) is widely used to treat infertility, yet accurate identification of euploid embryos remains challenging. While preimplantation genetic

[†] Shuangyi Tan and Xinxian Song contribute equally to this work.
[*] Corresponding authors are Zhen Li, Sibei Yang and Guanbin Li.

testing (PGT) can detect chromosomal abnormalities, it relies on invasive embryo biopsy and could be costly. Consequently, non-invasive euploidy prediction based on embryo morphology and developmental dynamics has attracted growing attention. With the development of time-lapse imaging technologies and deep learning, an increasing number of studies have explored embryo assessment models based on embryo developmental sequences [9, 4, 12, 14, 1]. Prior work has demonstrated the benefit of jointly exploiting spatial and temporal cues [21, 9], incorporating multi-focal morphological information [26, 24, 19, 8, 10], and integrating clinical features through late-stage fusion [22]. Despite these advances, most existing methods [15, 17, 23, 6] implicitly assume that developmental trajectories are synchronized across embryos and can be modeled within a unified representation space, leading to representations that primarily reflect population-level average patterns. Nevertheless, from biological perspectives, this assumption does not always hold. Embryo development is systematically influenced by clinical factors such as parental age, BMI, and sperm preservation methods, leading to substantial inter-individual variability in both developmental timing and morphological organization [5, 3, 2, 27]. Therefore, embryo development does not follow a single standardized trajectory, but rather exhibits diverse individual pathways around shared population-level patterns. **Ignoring such variability and modeling embryo development within a unified representation space may obscure embryo-specific morphological patterns and temporally critical stages, thereby limiting predictive reliability.**

Consequently, we revisit embryo euploidy prediction and propose a multi-level framework from the perspective of individualized modeling at three complementary levels. (1) At the morphological level, embryos may present distinct structural organizations even at the same developmental stage. We therefore model morphology as an adaptive combination of shared structural patterns conditioned on clinical context, enabling flexible characterization of embryo-specific spatial configurations while preserving common developmental regularities. (2) At the temporal level, embryos differ in developmental rhythm and stage importance. Instead of uniformly aggregating time points, we introduce individualized temporal importance modeling by learning embryo-conditioned stage-wise attention weights over sequential representations, enabling the model to highlight informative developmental phases and capture individualized temporal dynamics. (3) At the global level, embryos may deviate from typical developmental trajectories, reflecting trajectory-level instability beyond local spatial or temporal variations. We therefore learn sample-specific predictive variance from global embryo features and incorporate it into a heteroscedastic loss, where the classification term is inversely scaled by the estimated variance and regularized by a log-variance penalty. This mechanism automatically downweights embryos exhibiting large developmental deviation while preserving their contribution to learning, enabling a balanced modeling of population-level regularities and individual heterogeneity. Together, these designs bridge shared population patterns with embryo-specific variability across spatial, temporal, and global-level perspectives. In conclusion, the main contributions are summarized as follows:

1. We systematically review embryo euploidy prediction from the perspective of inter-individual variability and propose a multi-level individualized modeling framework that explicitly characterizes embryo individuality at three complementary levels: spatial morphology, temporal developmental dynamics, and global developmental reliability.
2. We construct a multi-modal embryo dataset integrating time-lapse imaging sequences with structured clinical information, enabling principled modeling of cross-modal embryo variability and individualized euploidy assessment.
3. Extensive experiments demonstrate that the proposed method achieves state-of-the-art performance for embryo euploidy prediction.

2 Data

We collaborated with the Reproductive Center of the First Affiliated Hospital of Sun Yat-sen University to collect a cohort of IVF embryo time-lapse videos together with corresponding clinical information for embryo development analysis. Embryos were cultured in two EmbryoScope incubators, each acquiring images from seven focal planes with a spatial resolution of 500×500 pixels. One incubator captured images at 10-minute intervals with a focal spacing of 25 or $15\mu m$, while the other recorded images every 15 minutes with a focal spacing of $15\mu m$. Embryo culture typically lasted 5–7 days. Chromosomal status were annotated by experienced embryologists based on PGT results.

In total, 1,034 embryos (517 euploid and 517 aneuploid) from 305 patients were collected. The dataset was randomly split at the patient level into training and test sets with an 8:2 ratio, corresponding to 246 and 59 patients, and 776 and 180 embryos, respectively. Embryos derived from the same parental couple were not split across the training and testing sets. To minimize potential bias caused by incubator-specific acquisition settings, embryos from the two incubator types were proportionally distributed across the training and test sets.

Based on prior clinical evidence [7, 2, 5, 3], we selected a set of clinical factors that are known to have a substantial impact on inter-embryo developmental variability. These factors include the ages of both partners, maternal body mass index (BMI), whether the sperm was cryopreserved, sperm retrieval method, and the presence of chromosomal translocations. For missing data handling, binary clinical variables were imputed with a value of -1 to indicate unknown status, while continuous variables were imputed using the mean values computed from the training set.

3 Method

We propose an individualized embryo euploidy prediction framework that explicitly models inter-embryo variability across three complementary levels: (i) morphological organization, (ii) temporal developmental dynamics, and (iii) global developmental context. An overview of the framework is shown in Fig. 1.

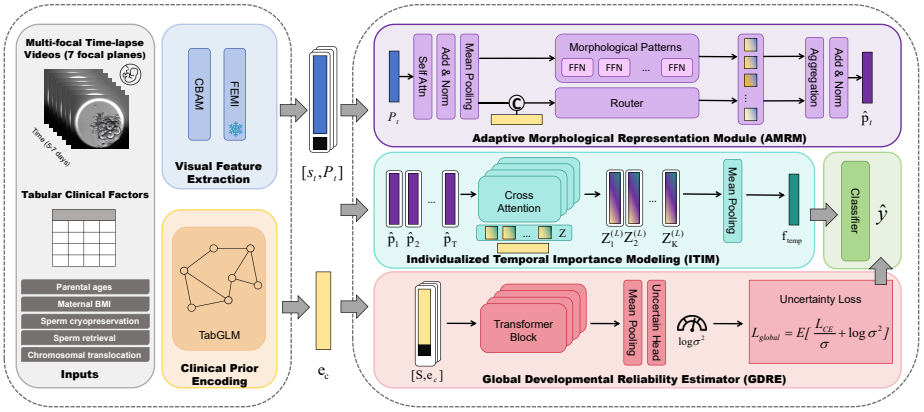

Fig. 1. Overview of the individualized embryo euploidy prediction framework.

3.1 Clinical Prior Encoding

Let $\mathbf{c} = [c_1, c_2, ..., c_6]$ denote the selected clinical variables, including parental ages, maternal BMI, sperm cryopreservation status, sperm retrieval method, and chromosomal translocation status. To effectively encode tabular clinical data that simultaneously contains numerical and categorical variables, and to capture the complex semantic and structural relationships among clinical factors, we adopt TabGLM [16] as the clinical prior encoder.

$$e_c = f_{TabGLM}(c) \tag{1}$$

3.2 Visual Feature Extraction

Embryo time-lapse images are captured at multiple focal planes, providing complementary spatial information across different depths.

Let $V = \{I_t^{(f)} | t = 1, ..., T, f = 1, ..., F\}$ denote the multi-focal time-lapse sequence, where F is the number of focal planes. we first aggregate the multi-focal observations at each time point using a CBAM-based [25] focal fusion module f_{CBAM}, which adaptively reweights focal-specific features via global average and max pooling, followed by residual fusion and channel reduction, before being tokenized for subsequent visual encoding:

$$\widetilde{I}_t = f_{CBAM}(\{I_t^{(f)}\}_{f=1}^{F}) \tag{2}$$

The fused frames $\{\widetilde{I}_t\}_{t=1}^{T}$ are then encoded using a frozen FEMI [20], which is a ViT backbone pretrained with 18 million time-lapse images:

$$[s_t, P_t] = f_{FEMI}(\widetilde{I}_t) \tag{3}$$

, where $s_t \in \mathbb{R}^C$ and $P_t \in \mathbb{R}^{N \times C}$ denote the frame-level global token and the patch-level embeddings, respectively.

3.3 Adaptive Morphological Representation Module (AMRM)

With different clinical contexts, embryos may exhibit distinct morphological organization even at the same developmental stage. Rather than assuming a single canonical morphological organization, we model embryo morphology as a clinical-prior combination of shared morphological patterns by our proposed Adaptive Morphological Representation Module (AMRM), allowing individual embryos to express distinct structural organizations.

Specifically, given the patch-level embeddings $P_t \in \mathbb{R}^{N\times C}$, we first apply self-attention (Attn) and residual normalization within each frame to capture spatial interactions among patches and then obtain a frame-level morphological representation p_t by aggregating patch features:

$$p_t = \frac{1}{N}\sum^{N} LN(P_t + Attn(P_t)),\ p_t \in \mathbb{R}^C \tag{4}$$

AMRM maintains M learnable morphological experts $\{\mathcal{E}_m(\cdot)\}_{m=1}^{M}$, which capture canonical morphological patterns shared across embryos. For each frame t, the model computes a set of combination weights by a routing function f_{router} conditioned on the frame-level morphology and clinical prior, which determine how strongly each expert contributes to the current morphological representation.

$$w_t = Softmax(f_{router}([p_t; e_c])),\ w_t \in \mathbb{R}^M \tag{5}$$

And the final morphology representation of t^{th} frame is:

$$\hat{p_t} = LN(p_t + \sum_{m=1}^{M} w_{t,m}\mathcal{E}_m(p_t)) \tag{6}$$

3.4 Individualized Temporal Importance Modeling (ITIM)

Embryos vary in developmental rhythm and stage importance, and treating all time points equally may obscure critical cues for euploidy prediction. Therefore, we introduce Individualized Temporal Importance Modeling (ITIM) to adaptively emphasize developmentally informative stages for each embryo.

Specifically, ITIM maintains K learnable temporal queries $Z^{(0)} = \{z_k\}_{k=1}^{K}$ with $z_k \in \mathbb{R}^C$. To incorporate embryo-specific prior information, the temporal queries are biased using the clinical prior embedding:

$$Z^{(0)} \leftarrow Z^{(0)} + \Phi(e_c) \tag{7}$$

, where $\Phi(e_c)$ denote linear projection for alignment. The speciallized queries then interact with morphology-aware frame representations $\hat{P} = \{\hat{p_1}, \hat{p_2}, ..., \hat{p_T}\}$ through a stack of cross-attention layers (l denote the l^{th} layer):

$$Z^{(l+1)} = Attn(Z^{(l)}, \hat{P}, \hat{P}) \tag{8}$$

After L layers, the embryo-level temporal representation is obtained by:

$$f_{temp} = \frac{1}{K} \sum_{k=1}^{K} Z_k^{(L)} \tag{9}$$

Additionally, to avoid redundancy among temporal modeling components and promote complementary temporal perspectives, we impose a diversity constraint on the temporal queries:

$$L_{div} = \frac{1}{K(K-1)} \sum_{i \neq j} |cos(z_i, z_j)| \tag{10}$$

3.5 Global Developmental Reliability Estimator (GDRE)

At the global level, embryo euploidy prediction should account for how reliably population-level developmental patterns manifest in each individual embryo. We therefore introduce Global Developmental Reliability Estimator (GDRE) to estimate embryo-specific developmental reliability and adaptively modulate the influence of individual embryos during optimization, balancing shared global regularities with individual deviations. Concretely, GDRE operates on the sequence of frame-level global tokens $S = \{s_t\}_{t=1}^{T}$. A temporal Transformer is employed to model long-range developmental dynamics under embryo-specific clinical context by concatenating the clinical prior embedding e_c to each time step, and the resulting sequence representation is temporally aggregated to obtain a compact global developmental summary:

$$f_{global} = \frac{1}{T} \sum_{t=1}^{T} Transformer([S; e_c]) \tag{11}$$

Rather than directly using this representation for classification, GDRE maps the global summary to a scalar sample-dependent reliability indicator:

$$log\ \sigma^2 = h(f_{global}) \tag{12}$$

where σ^2 reflects the model's confidence in the developmental evidence provided by the current embryo. Importantly, this reliability estimate is not supervised explicitly, but is learned jointly with the prediction task. Given the predicted class logits $\hat{y}$, the true label y and the estimated reliability σ, we adopt a heteroscedastic formulation of the classification loss:

$$L_{global} = \mathbb{E}[\frac{L_{CE}(\hat{y}, y)}{\sigma} + log\ \sigma^2] \tag{13}$$

This objective allows the model to adaptively regulate the influence of each embryo during training based on its intrinsic developmental characteristics. It complements the fine-grained individualized modeling performed by AMRM and ITIM by operating at the level of the entire developmental trajectory.

3.6 Loss Functions

The total loss function is combined with the original CLIP loss of TabGLM, the diversity loss of ITIM and the reformed heteroscedastic classification loss:

$$L_{total} = \alpha * L_{global} + \beta * L_{TabGLM} + \gamma * L_{div} \tag{14}$$

4 Experiment

4.1 Implementation Details

The model was implemented using PyTorch and trained on a single NVIDIA RTX 3090 GPU. Optimization was performed with Adam [13] using a learning rate of 2×10^{-5} and a batch size of 4. For temporal efficiency, uniform sampling was applied by dividing each video into $n = 16$ equal segments and randomly selecting one frame from each segment during training. The loss weights were fixed as $\alpha = 0.8$, $\beta = 0.2$ and $\gamma = 0.05$ across all experiments.

4.2 Experiment Result Analysis

We compared our method with state-of-the-art methods, including representative single-modal and multi-modal approaches, on two time-lapse incubators (868 and 869) and their mixture (mix) for embryo euploidy prediction. For a fair comparison, we implemented all methods following their officially proposed architextures under identical protocols. As shown in Table 1, our proposed framework achieves the state-of-the-art performance across all settings, introducing a personalized euploidy prediction approach tailored to embryo-specific characteristics, explicitly modeling inter-embryo heterogeneity. On mix, compared with the second-best method, it achieves relative improvements of 0.54% in Acc, 4.08% in AUC, and 13.28% in F1, demonstrating stronger discrimination ability.

Table 1. External comparisons with state-of-the-art methods on two time-lapse incubators (868 and 869) and their mixture (mix).

Model	Multi-modal	mix			868			869		
		Acc	AUC	F1	Acc	AUC	F1	Acc	AUC	F1
CoSTeM[21]	×	0.710	0.774	0.708	0.720	0.802	0.731	0.705	0.727	0.566
FEMI[20]	×	0.620	0.759	0.679	0.656	0.791	0.695	0.589	0.753	0.659
AMSNet[26]	×	0.706	0.739	0.662	0.716	0.802	0.764	0.602	0.592	0.311
ResNet-GRU[11]	×	0.705	0.747	0.605	0.705	0.772	0.693	0.653	0.692	0.584
MMIVF[12]	✓	0.650	0.662	0.577	0.650	0.730	0.578	0.640	0.590	0.575
ATRI-Net[22]	✓	0.740	0.784	0.655	0.676	0.777	0.703	0.590	0.653	0.429
DFNet[18]	✓	0.630	0.673	0.697	0.686	0.743	0.746	0.525	0.566	0.602
Our model	✓	**0.744**	**0.816**	**0.742**	**0.725**	**0.823**	**0.772**	**0.744**	**0.782**	**0.667**

Table 2. Ablation study on structural modules and clinical prior integration.

AMRM	GDRE	ITIM	Clinical Prior Integration	Acc	AUC	F1
✓			All	0.706	0.724	0.624
✓	✓		All	0.711	0.747	0.683
✓	✓	✓	None	0.705	0.728	0.638
✓	✓	✓	AMRM	0.706	0.787	0.639
✓	✓	✓	AMRM + GDRM	0.728	0.804	0.642
✓	✓	✓	All	0.744	0.816	0.742

Specifically, this advantage consistently carries over to individual incubators. On 868 and 869, our model again attains the best performance, surpassing the second-best method CoSTeM by 0.69%/5.53% in Acc, 2.62%/7.57% in AUC, and 5.61%/17.85% in F1, respectively. Overall, these results indicate that the proposed framework generalizes well across different time-lapse incubators and remains robust under incubator-specific distribution shifts.

4.3 Ablation Study

To systematically evaluate the contribution of each component, we conduct ablation experiments on the three individualized modeling modules as well as different strategies for clinical prior integration (Table 2).

We first analyze the progressive introduction of the three structural modules. Introducing GDRE on top of AMRM improves AUC from 0.724 to 0.747, indicating that modeling global developmental deviation provides complementary information beyond morphology. Further adding ITIM increases AUC to 0.816 and F1 to 0.742, indicating that modeling embryo-specific stage importance provides complementary temporal cues for euploidy prediction. These results confirm that individualized modeling at morphological, temporal, and global levels contributes synergistically.

We then investigate how clinical prior information interacts with the structural modules. Removing clinical prior leads to a clear performance drop, with AUC decreasing to 0.728, indicating that visual signals alone are insufficient. Progressively injecting clinical information into AMRM and GDRE further improves performance, increasing AUC from 0.787 to 0.804. When clinical prior is fully integrated, the model achieves the best results, reaching an AUC of 0.816 and an F1 score of 0.742, which demonstrate that clinical prior consistently enhances individualized modeling at multiple levels.

5 Conclusion

In this work, we revisit embryo euploidy prediction from the perspective of individualized modeling. Rather than assuming a unified developmental trajectory, the proposed framework characterizes embryo variability at morphological, temporal, and global levels, while integrating clinical prior information to modulate

representation learning. By balancing shared developmental regularities with embryo-specific deviations, our model achieves superior predictive performance and demonstrates the importance of multi-level individualized modeling for reliable and clinically meaningful euploidy assessment.

Acknowledgments. This work is supported in part by the National Natural Science Foundation of China (No. 62322608) and the National Natural Science Foundation of China under Grant (No.62576365) and in part by the GuangDong Basic and Applied Basic Research Fund (NO. 2024A1515010255) and in part by Sun Yatsen University Clinical Medicine Research 5010 Program (NO. 2023003).

Disclosure of Interests. The authors have no competing interests to declare that are relevant to the content of this article.

References

1. Borna, M.R., Sepehri, M.M., Maleki, B.: An artificial intelligence algorithm to select most viable embryos considering current process in ivf labs. Frontiers in artificial intelligence **7**, 1375474 (2024)
2. Bruno, C., Bourredjem, A., Barry, F., Frappier, J., Martinaud, A., Chamoy, B., Hance, I., Ginod, P., Cavalieri, M., Amblot, C., et al.: Analysis and quantification of female and male contributions to the first stages of embryonic kinetics: study from a time-lapse system. Journal of Assisted Reproduction and Genetics **39**(1), 85–95 (2022)
3. Cannarella, R., Leanza, C., Chamayou, S., Crafa, A., Barbagallo, F., Guglielmino, A., La Vignera, S., Calogero, A.E.: Impact of male factors on morphokinetic parameters: a prospective analysis using time-lapse monitored embryos. Journal of Assisted Reproduction and Genetics **42**(10), 3551–3560 (2025)
4. Chen, T., Cheng, Y., Wang, J., Yang, Z., Zheng, W., Chen, D.Z., Wu, J.: Automating blastocyst formation and quality prediction in time-lapse imaging with adaptive key frame selection. In: International Conference on Medical Image Computing and Computer-Assisted Intervention. pp. 445–455. Springer (2022)
5. Elkhatib, I., Nogueira, D., Bayram, A., Abdala, A., Ata, B., Melado, L., Lawrenz, B., Kalafat, E., Gianaroli, L., Fatemi, H.M.: The influence of male age and sperm parameters on blastulation and euploidy rates. Fertility and Sterility (2025)
6. Eswaran, M., Balasubramanie, P., Salman, J.M.: Deep learning algorithms for time-lapse image sequence-based automated blastocyst quality detection. In: 2023 4th International Conference on Electronics and Sustainable Communication Systems (ICESC). pp. 1246–1252. IEEE (2023)
7. Ezoe, K., Miki, T., Akaike, H., Shimazaki, K., Takahashi, T., Tanimura, Y., Amagai, A., Sawado, A., Mogi, M., Kaneko, S., et al.: Maternal age affects pronuclear and chromatin dynamics, morula compaction and cell polarity, and blastulation of human embryos. Human Reproduction **38**(3), 387–399 (2023)
8. Handayani, N., Danardono, G.B., et al.: Improving deep learning-based algorithm for ploidy status prediction through combined u-net blastocyst segmentation and sequential time-lapse blastocysts images. Journal of Reproduction & Infertility **25**(2), 110 (2024)

9. He, C., Karpavičiūtė, N., Hariharan, R., Jacques, C., Chambost, J., Malmsten, J., Zaninovic, N., Wouters, K., Fréour, T., Hickman, C., et al.: Embryo graphs: Predicting human embryo viability from 3d morphology. In: International Conference on Medical Image Computing and Computer-Assisted Intervention. pp. 80–90. Springer (2024)
10. He, H., Wu, L., et al.: A novel non-invasive embryo evaluation method (nics-timelapse) with enhanced predictive precision and clinical impact. Heliyon **10**(9) (2024)
11. Kalyani, K., Deshpande, P.S.: A deep learning model for predicting blastocyst formation from cleavage-stage human embryos using time-lapse images. Scientific Reports **14**(1), 28019 (2024)
12. Kim, J., Shi, Z., Jeong, D., Knittel, J., Yang, H.Y., Song, Y., Li, W., Li, Y., Ben-Yosef, D., Needleman, D., et al.: Multimodal learning for embryo viability prediction in clinical ivf. In: International Conference on Medical Image Computing and Computer-Assisted Intervention. pp. 542–552. Springer (2024)
13. Kingma, D.P.: Adam: A method for stochastic optimization. arXiv preprint arXiv:1412.6980 (2014)
14. Kragh, M.F., Rimestad, J., Berntsen, J., Karstoft, H.: Automatic grading of human blastocysts from time-lapse imaging. Computers in biology and medicine **115**, 103494 (2019)
15. Lockhart, L., Saeedi, P., Au, J., Havelock, J.: Automating embryo development stage detection in time-lapse imaging with synergic loss and temporal learning. In: International Conference on Medical Image Computing and Computer-Assisted Intervention. pp. 540–549. Springer (2021)
16. Majee, A., Xenochristou, M., Chen, W.P.: Tabglm: Tabular graph language model for learning transferable representations through multi-modal consistency minimization. In: Proceedings of the AAAI Conference on Artificial Intelligence. vol. 39, pp. 19387–19395 (2025)
17. Ou, Z., Zhang, Q., Li, Y., Meng, X., Wang, Y., Ouyang, Y., Li, Z., Zeng, K.: Classification of human embryos by using deep learning. In: International Conference on Cloud Computing, Performance Computing, and Deep Learning (CCPCDL 2023). vol. 12712, pp. 342–347. SPIE (2023)
18. Ouyang, X., Wei, J., Huo, W., Wang, X., Li, R., Zhou, J.: Defusion: An effective decoupling fusion network for multi-modal pregnancy prediction. arXiv preprint arXiv:2501.04353 (2025)
19. Rajendran, S., Brendel, M., Barnes, J., Zhan, Q., Malmsten, J.E., Zisimopoulos, P., Sigaras, A., Ofori-Atta, K., Meseguer, M., Miller, K.A., et al.: Automatic ploidy prediction and quality assessment of human blastocysts using time-lapse imaging. Nature Communications **15**(1), 7756 (2024)
20. Rajendran, S., Rehani, E., Phu, W., Zhan, Q., Malmsten, J.E., Meseguer, M., Miller, K.A., Rosenwaks, Z., Elemento, O., Zaninovic, N., et al.: A foundational model for in vitro fertilization trained on 18 million time-lapse images. Nature Communications **16**(1), 6235 (2025)
21. Sun, Y., Wang, Y., Shi, J., Zhang, Z., Xiao, Y., Zhu, L., Jiang, M., Nie, Q.: Time-lapse video-based embryo grading via complementary spatial-temporal pattern mining. In: International Conference on Medical Image Computing and Computer-Assisted Intervention. pp. 594–604. Springer (2025)
22. Tan, S., Liang, Z., Li, M., Yang, S., Li, Z., Mai, Q., Li, G.: Atri-net: A multimodal and multifocal fusion network for embryo euploidy prediction. In: 2026 IEEE 23th International Symposium on Biomedical Imaging (ISBI). pp. 1–5. IEEE (2026)

23. Truong, V.V., Le, M.H., Phu, P.L., Phan, H., Le, T., Nguyen, H., Pham, V.D., Le, X.H.: A deep learning approach to embryo quality assessment. In: The International Conference on Intelligent Systems & Networks. pp. 452–461. Springer (2024)
24. Wang, S., Zhou, C., Zhang, D., Chen, L., Sun, H.: A deep learning framework design for automatic blastocyst evaluation with multifocal images. IEEE Access **9**, 18927–18934 (2021)
25. Woo, S., Park, J., Lee, J.Y., Kweon, I.S.: Cbam: Convolutional block attention module. In: Proceedings of the European conference on computer vision (ECCV). pp. 3–19 (2018)
26. Xie, X., Yan, P., Cheng, F.Y., Gao, F., Mai, Q., Li, G.: Early prediction of blastocyst development via time-lapse video analysis. In: 2022 IEEE 19th International Symposium on Biomedical Imaging (ISBI). pp. 1–5. IEEE (2022)
27. Ye, D., Ye, Z., Zhang, H.: Effects of sperm dna fragmentation on embryo morphokinetic parameters and laboratory outcomes in women of different ages during intracytoplasmic sperm treatment cycles. Archives of Gynecology and Obstetrics pp. 1–6 (2025)